Antioxidant potential and increased photocatalytic efficiency of gallic acid capped ZnO and NiO NPs for azo dyes degradation: Effect of heterojunction coupling and machine learning-assisted modeling

Aqeela Sikandar, [a] Abu Bakar Siddique, *[a] Azhar Abbas, [a,b] Abdul Majid, [c] Bilal Sikandar,[d] Muhammad Ashraf Shaheen,[e] Umar Nishan,[f] Khaled Fahmi Fawy [g]

[a] *Institute of Chemistry, University of Sargodha, Sargodha 40100, Pakistan*

[b] *Department of Chemistry, Government Ambala Muslim College, Sargodha 40100, Pakistan*

[c] *Department of Botany, University of Sargodha, Sargodha 40100, Pakistan*

[d] *Department of Physics and Applied Mathematics, Pakistan Institute of Engineering and Applied Sciences (PIEAS), Nilore, Islamabad 45650, Pakistan*

[e] *Department of Allied Health Sciences, The Superior University Lahore, Sargodha-Campus 40100, Pakistan*

[f] *Department of Chemistry, Kohat University of Science and Technology, Kohat 26000 KP, Pakistan*

[g] *Department of Chemistry, Faculty of Science, Research Center for Advanced Materials Science (RCAMS), King Khalid University, P.O. Box 960, Abha, 61421, Saudi Arabia.*

Corresponding Author:

Dr. Abu Bakar Siddique: *Institute of Chemistry, University of Sargodha, Sargodha 40100, Pakistan.* abubakar.siddique@uos.edu.pk & abubakar054@gmail.com

S1. Instruments Used

The XRD spectrum was obtained using the JDX-3532 diffractometer from JEOL, Japan, utilizing Cu-Kα radiation (wavelength of 1.5418 Å) in a 2θ range of 20–80°. FTIR analysis was conducted using a Shimadzu FTIR-8400S spectrophotometer (Japan), and absorbance spectra were obtained with a Shimadzu UV-1800 spectrophotometer (Japan). Morphological analysis of samples was performed utilizing SEM with the JSM5910 equipment from JEOL, Japan.

S2. Antioxidant activity assays

2.1. DPPH radical scavenging assay

In the DPPH test, the radical scavenging efficiency of the nanoparticles and nanocomposites was measured in comparison to ascorbic acid as the reference. Sample solutions ranging in concentration from 100 to 500 µg/mL were added to 3 mL of a DPPH ethanolic solution (prepared by dissolving 4 mg DPPH in 100 mL ethanol). After 30 minutes of dark incubation, the absorbance was recorded at 517 nm, and the scavenging percentage was calculated.

2.2. TPC assay

For the TPC assay, nanoparticle solutions (100–500 µL at 1 mg/mL) were combined with 250 µL of 1N Folin-Ciocalteu reagent and diluted in 2 mL of distilled water. Next, 750 µL of 20% sodium carbonate was added, followed by dilution with distilled water to a final volume. After a 30-minute incubation, absorbance was measured at 765 nm, and results were reported in terms of gallic acid equivalents (µg GAE/mL).

2.3. FRAP assay

The FRAP assay involved preparing the reagent by mixing 300 mM acetate buffer (pH 3.6), 10 mM TPTZ in 40 mM HCl, and 20 mM $FeCl_3 \cdot 6H_2O$ in a 10:1:1 ratio. The reagent was preheated

to 37°C before use. Each nanoparticle sample (100 µL, at 100–500 µg/mL concentration) was added to 3 mL of the FRAP reagent and incubated at 37°C for 30 minutes in the dark. The absorbance was then read at 593 nm, and antioxidant activity was quantified using a gallic acid calibration curve, expressed as µg GAE/mL.

S3. Butler–Ginley method

Butler–Ginley equations (**Equation i-ii**) were used to calculate potentials of conduction and valence bands.

$$E_{CB} = X - E_e - \frac{1}{2}E_g \qquad (i)$$

$$E_{VB} = E_{VB} + E_g \qquad (ii)$$

Where:

X = Absolute electronegativity of the semiconductor (in eV) = 5.71 eV for ZnO and 5.60 for NiO

E_e = Energy of free electrons on the hydrogen scale = 4.50 eV

E_g = Band gap (in eV) = 3.14 eV for ZnO NPs and 2.78 eV for NiO NPs

S4. Mechanism of Photodegradation of dyes

$$g - ZnO - NiO\,NCs + h\upsilon(UV - Vis) \rightarrow g - ZnO - NiO\,NCs(e^-(CB) + h^+(VB)) \qquad (a)$$

$$2H_2O(ads) + h^+(VB) \rightarrow OH^\bullet(ads) + H_3O^+(ads) \qquad (b)$$

$$O_2 + e^-(CB) \rightarrow O_2^{\bullet -}(ads) \qquad (c)$$

$$2HOO^\bullet(ads) \rightarrow H_2O_2(ads) + O_2 \qquad (d)$$

$$H_2O_2(ads) \rightarrow 2OH^\bullet(ads) \qquad (e)$$

$$Azo\,dye + 2OH^\bullet \rightarrow \text{intermediates} \rightarrow CO_2 + H_2O \qquad (f)$$

$$Azo\,dye + h^+(VB) \rightarrow \text{Oxidation Products} \qquad (g)$$

$$Azo\,dye + e^-(CB) \rightarrow \text{Reduction Products} \qquad (h)$$

Table S1. Dataset overview showing pH variation, respective fixed conditions and experimental degradation efficiency.

pH	Catalyst Dose (mg)	Initial concentration of dye (ppm)	Azo Dye	Degradation (%)
2	50	10	CV	46
4	50	10	CV	68
6	50	10	CR	72

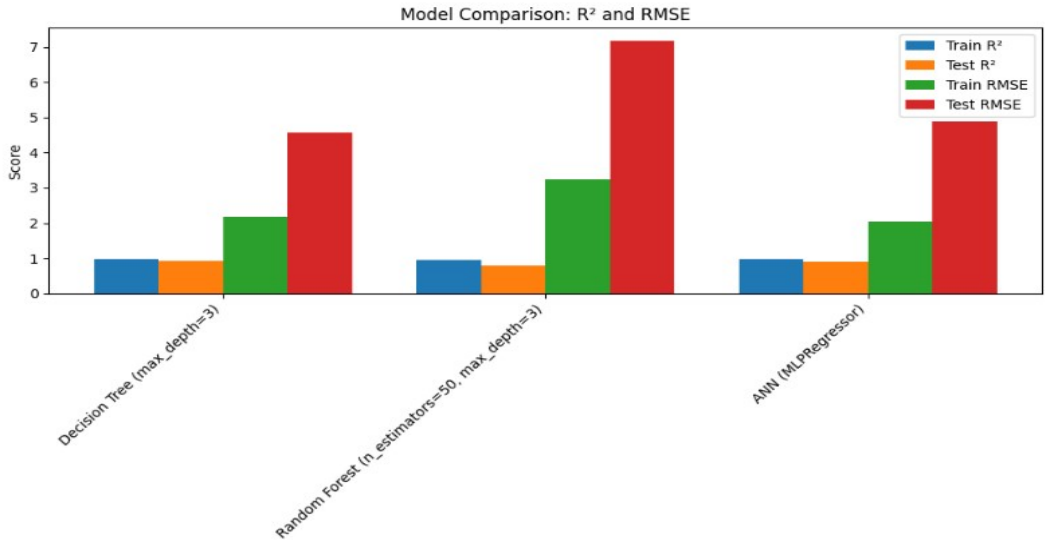

Figure S1. Comparison model of R^2 and RMSE of various models (ANN, decision tree and random forest) with best fitting of Decision Tree (max_depth=3) for optimization of pH

Table S2. Summary of the dataset illustrating variation in catalyst dose with corresponding fixed conditions and experimental degradation efficiency.

pH	Catalyst Dose (mg)	Initial concentration of dye (ppm)	Azo Dye	Degradation (%)
8	5	10	CV	48
8	10	10	CV	64
8	20	10	CR	68

Table S3. Comparison of performance of ML models in prediction of degradation efficiency for values of catalyst dose.

Model	Training set			Testing set		
	R^2	RMSE	MAE	R^2	RMSE	MAE
Decision Tree	0.970	2.288	1.577	0.875	4.661	3.671
Random Forest	0.963	2.529	2.000	0.864	4.864	4.161
ANN	0.942	3.169	1.941	0.769	6.340	4.104

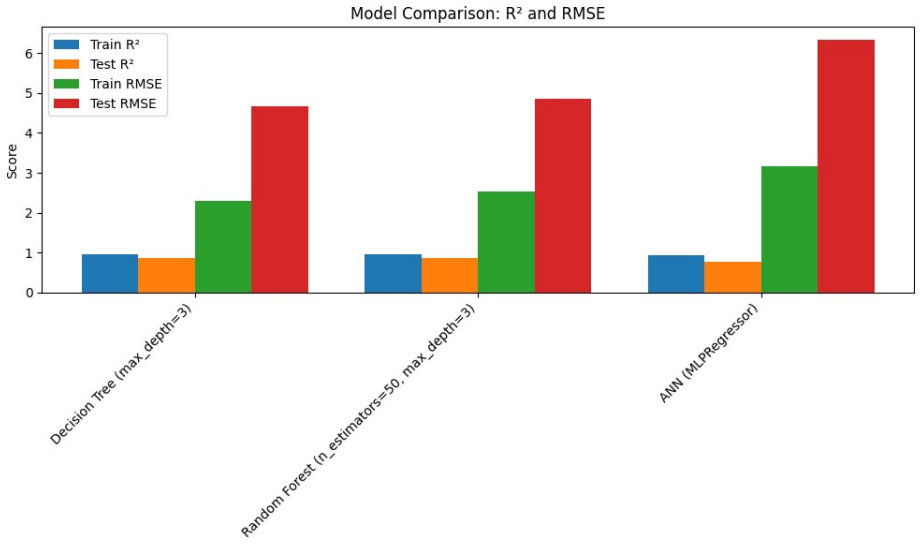

Figure S2. Comparison model of R^2 and RMSE of various models (ANN, decision tree and random forest) with best fitting of Decision Tree (max_depth=3) for optimization of catalyst dose

Table S4. Summary of the dataset illustrating variation in initial dye concentration with corresponding fixed conditions and experimental degradation efficiency.

pH	Catalyst Dose (mg)	Initial concentration of dye (ppm)	Azo Dye	Degradation (%)
8	50	10	CV	95
8	50	20	CV	79
8	50	30	CR	77

Table S5. Dataset overview illustrating variation in catalyst dose with associated fixed conditions and experimental degradation efficiency

Model	Training set			Testing set		
	R^2	RMSE	MAE	R^2	RMSE	MAE
Decision Tree	0.999	0.278	0.155	0.885	3.763	2.863
Random Forest	0.989	1.188	0.911	0.915	3.225	3.000
ANN	0.997	0.641	0.480	0.943	2.647	2.318

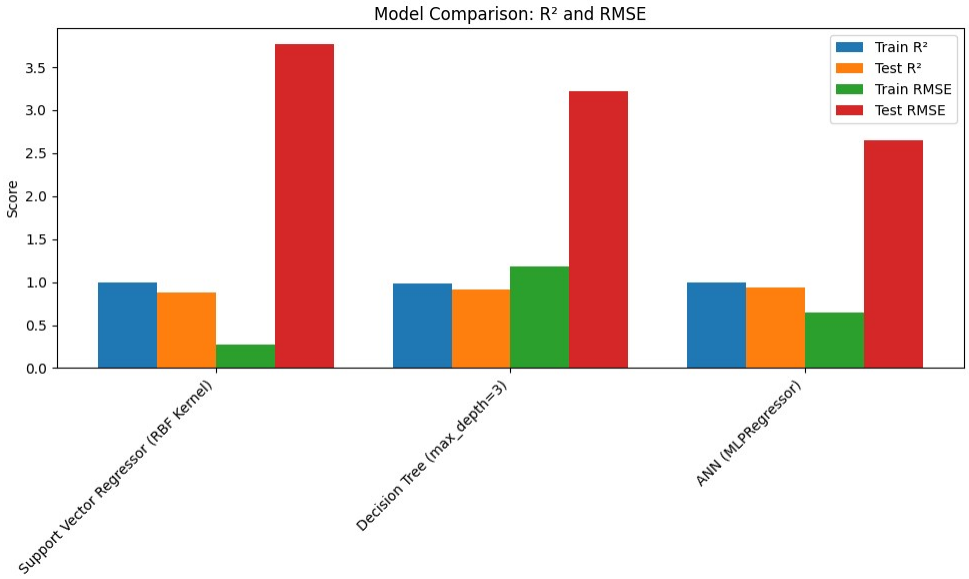

Figure S3. Comparison model of R^2 and RMSE of various models (ANN, decision tree and random forest) with best fitting of ANN for optimization of initial dye concentration